Naval Information Warfare Center PACIFIC

TECHNICAL REPORT 3258
JANUARY 2022

Advanced Electronic Films Using Pulsed Laser Deposition: Multi-component Film Composition Control

W. C. McGinnis
Alexandru Hening
Teresa Emery-Adleman
NIWC Pacific

Naval Information Warfare Center Pacific (NIWC Pacific)
San Diego, CA 92152-5001

This page is intentionally blank.

TECHNICAL REPORT 3258
JANUARY 2022

Advanced Electronic Films Using Pulsed Laser Deposition: Multi-component Film Composition Control

W. C. McGinnis
Alexandru Hening
Teresa Emery-Adleman
NIWC Pacific

Administrative Notes:
This report was approved through the Release of Scientific and Technical Information (RSTI) process in May 2021 and formally published in the Defense Technical Information Center (DTIC) in January 2022.

NIWC Pacific
San Diego, CA 92152-5001

NIWC Pacific
San Diego, California 92152-5001

A. D. Gainer, CAPT, USN
Commanding Officer

W. R. Bonwit
Executive Director

ADMINISTRATIVE INFORMATION

This report was authored in 2018 and the content represents work performed by the Intelligent Sensing Branch (Code 71740) of the Basic and Applied Research Division, SPAWAR Systems Center Pacific (SSC Pacific), San Diego, CA. SSC Pacific formally changed its name to Naval Information Warfare Center Pacific (NIWC Pacific) in February 2019.

Released by
Ayax Ramirez, Division Head
Basic and Applied Research Division

Under authority of
Stephen Russell, Department Head
Cyber / Science & Technology Department

ACKNOWLEDGMENTS

The authors gratefully acknowledge the support of the SSC Pacific Innovative Independent Program (IIP) for the In-house Laboratory Independent Research (ILIR) project “Advanced Electronic Films using Pulsed Laser Deposition.” The authors also thank the following individuals for their contributions to and support of the project:

- Dr. Manjit Randhawa, visiting professor under the Office of Naval Research (ONR) Summer Faculty Research Program, Southern University and A&M College, Baton Rouge
- Dr. Adi Bulsara, SSC Pacific Code 71000

Editor: MRM

EXECUTIVE SUMMARY

OBJECTIVE

Demonstrate a proof-of-concept magnetic field sensor using optimized multiferroic $Bi_xDy_{1-x}FeO_3$ (BDFO) films grown by pulsed laser deposition (PLD) while controlling atomic composition of the films using a single, split-composition target.

RESULTS TO DATE

A simple means of controlling the elemental composition of BDFO films has been demonstrated. Using a conventional single-composition PLD ablation target, the film composition can be difficult to control, particularly for films deposited onto heated substrates, when the target contains some elements that are relatively more volatile than others.

The method described in this report uses a split ablation target that is rotated about its center (to maximize target usage or coverage, and to more uniformly ablate the target surface) combined with variable speed laser beam rastering across the target. By using different raster speeds over the course of the raster cycle, the beam can spend more time on one half of the split target than on the other half, compensating for any loss due to evaporation from the heated substrate.

This film composition control technique was demonstrated by both simple model calculations of the laser beam raster position versus time (from which the beam dwell times were calculated) and by measurement of the elemental composition of a series of BDFO films deposited with various beam raster settings. Electrical hysteresis measurements show that the initial films are ferroelectric, despite having non-optimal elemental composition.

FUTURE PLANS

Using the demonstrated film composition control technique, a series of BDFO films with a composition close to $Bi_{0.7}Dy_{0.3}FeO_3$ will be deposited to determine the film stoichiometry that results in multiferroic properties best suited for application to a magnetic field sensor. A proof-of-concept sensor will be constructed and demonstrated using these optimized BDFO films.

Future work also includes controlling the elemental and structural composition of deposited thin films by using a radio frequency (rf) plasma-assisted pulsed laser deposition technique. The addition of an rf discharge to the PLD system allows for tuning of the deposited layer's crystalline phase and orientation, dependent on the specific type and energy of the species involved in the discharge (oxygen, nitrogen).

This page is intentionally blank.

ACRONYMS

BDFO	$Bi_xDy_{1-x}FeO_3$
EDS	Energy dispersive spectroscopy
ONR	Office of Naval Research
PLD	Pulsed laser deposition
SPAWAR	Space and Naval Warfare
SSC	SPAWAR Systems Center
WDS	Wavelength dispersive spectroscopy

This page is intentionally blank.

CONTENTS

FIGURES

TABLES

1. INTRODUCTION

1.1 PROBLEM ADDRESSED

This report includes results to date on research to demonstrate a proof-of-concept magnetic field sensor based on optimized multiferroic $Bi_xDy_{(1-x)}FeO_3$ (BDFO) films grown by pulsed laser deposition (PLD) using a split ablation target. A multiferroic material is one that is both ferroelectric and ferromagnetic [1]. A single split target is used to achieve the desired elemental composition in the BDFO film by setting different ablation dwell times for each target half (where each half has a different atomic ratio of Bi, Dy, and Fe). The measured film composition, crystal structure, and electronic/magnetic properties are used to test the validity of this film composition control method.

A variety of new and technologically useful thin films, including ferroelectric, multiferroic, and high-temperature superconductor films, can be produced with this split-target PLD technique. Such films are needed for improved sensor, electronic, photonic, spintronic, and MEMS devices for application to next generation Navy systems in the quest to achieve information dominance.

1.2 BACKGROUND

Pulsed laser deposition is commonly used to grow chemically complex thin films (by laser ablation of a target material) that are difficult or impossible to produce by traditional methods. When depositing dissimilar chemical elements onto heated substrates, the target and resultant film target often have different elemental compositions. Usually, multiple targets with various compositions are used, on a trial and error basis, to achieve the desired film composition. A single split ablation target can be used instead to grow films with the needed composition (or films with a variety of compositions) by setting different ablation dwell times for each target half.

1.3 PROJECT PERSONNEL

The primary SSC Pacific personnel working on this project are principal investigator Dr. Wayne McGinnis and co-investigators Dr. Alexandru Hening and Dr. Teresa Emery-Adleman. Dr. Manjit Randhawa (visiting professor under the ONR Summer Faculty Research Program from Southern University and A&M College, Baton Rouge) helped develop and test a circuit to be used for detecting weak, low-frequency magnetic fields (composed of three coupled Sawyer-Tower sub-circuits) using multiferroic films as the field-sensitive element. This approach is based on the non-linear dynamics theories developed at SSC Pacific by Dr. Adi Bulsara, who also provided financial support through ONR for Dr. Randhawa's visits.

This page is intentionally blank.

2. APPROACH AND METHODS

2.1 ABLATION TARGETS

2.1.1 Split Target Method

One often heralded advantage of PLD for growth of chemically complex materials is stoichiometric transfer of the target material to the substrate that supports the deposited film. In some cases, though, target stoichiometry is preserved only under very specific deposition conditions that vary depending on the target material and the substrate temperature. Such conditions are often difficult and time-consuming to determine.

Previous methods used to address this problem include: (1) use of multiple ablation targets (on a trial-and-error basis) to determine the exact target composition needed to produce the desired film composition, (2) use of a split target (or two separate single-composition targets), with different laser dwell times on each target half (by alternatively ablating each target half, spending a different amount of time on each half), and (3) use of a split or sectioned target that is rotated around a point not coincident with the target center (varying the distance between the rotation point and the target center to achieve various film compositions).

Method 1 is time consuming and expensive, requiring the manufacture or purchase of numerous targets of various compositions. Method 2, if implemented without target rotation and laser beam or target rastering, can result in alternating layers of the target material halves, requiring post-deposition annealing to achieve a homogeneous film, and non-uniform target surface usage. Method 3 requires a special mechanism for the off-target-center rotation (or a smaller target than would be used for on-target-center rotation) and does not incorporate laser beam or target rastering to maximize target surface usage and ablation uniformity.

Method 2 uses a split (or multi-section) ablation target that is rotated about its center (to maximize target usage or coverage, and to more uniformly ablate the target surface) combined with a laser beam that is rastered across the target [2]. Over the course of the raster cycle (and the deposition), the laser beam spends more time on one half of the split target than on the other half. The split target is constructed so that one half contains more of the most volatile element being deposited than the other half. Using growth of a BiFeO3 film as an example, one target half might have a 2:1 atomic ration of Bi to Fe, while the other half has a 1:1 atomic ratio of these elements. By spending more or less time on the Bi-rich target side, the laser beam will ablate more or less bismuth, resulting in a film with a higher or lower Bi:Fe ratio, respectively.

This split-target composition control technique was first attempted using “fast” target rotation (that is, with the beam hitting the surface of each target half multiple times during the course of a single beam raster cycle). This method was explored using both simple model calculations of the laser beam raster position versus time (giving the beam dwell times) and by measurement of the elemental composition of a series of BDFO films deposited with various beam raster settings (target rotation speed of 10 rpm).

It became apparent that the target rotation and beam raster motions do not stay synchronized over the course of the film deposition time (about one hour), and therefore the beam dwell times on each target half (and resulting film composition) can change as the deposition progresses. To address this issue, a method using “slow” target rotation (where the target undergoes at most 1/2 revolution during the entire deposition process) was modeled and implemented. A typical “slow” target rotation speed is 0.005 rpm, or 0.3 revolutions per hour.

2.1.2 Modeling and Simulation

Simultaneous target rotation and beam rastering were first attempted as a laboratory simulation (inside the PLD chamber) using a paper circle (with semicircular sides marked as “1” and “2”) as a “target” and a rastered low-power red laser. Numbered frame shots from a video recording of the rotation and raster motions are shown in Figure 1. The beam starts at the target center (frame 1),

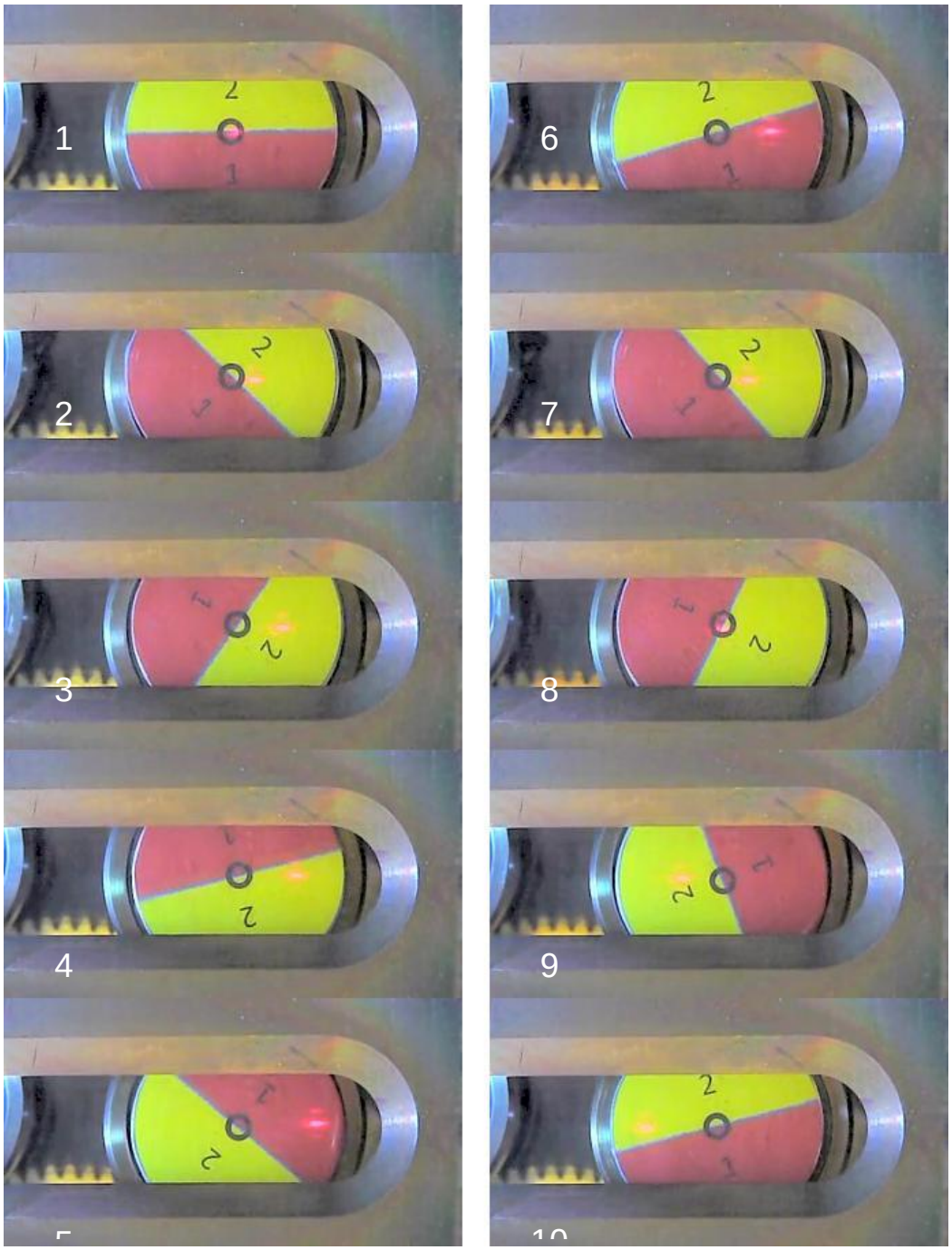

Figure 1. Simulated target rotation with simultaneous laser beam (red dot) rastering.

rastering right (frames 2-5) and then left (frames 6-10), while the target rotates at 10 rpm in a clockwise direction.

A spreadsheet was used to calculate the expected fraction of time that the rastered laser beam would spend on each half of a rotating split target (dwell time). The reference directions and target rotation angle are defined as shown in Figure 2. For calculation purposes, the target rotation was broken up into discrete 10° steps, covering two complete revolutions of the target (720°). The target rotational position is specified by the angular displacement θ measured between the laser beam plane and the boundary line separating the two target halves. The laser beam was rastered (in this model calculation) back and forth across the target diameter, starting at the target center, reversing direction before reaching the target edge, returning to the target center at a specified value $\theta = \theta_1$, continuing on to near the opposite target edge, and returning again to the target center when $\theta = \theta_2 = 720°$. For a given target rotational speed (typically 10 rpm), the beam raster speed needed for each segment of beam motion was calculated, along with the beam position along the target diameter (with a constant raster speed within each segment). In this model, the beam is assumed to intersect the target surface as a point (no beam width). Based on the calculated beam position at each 10° interval, the fraction of time that the beam spent on each target half was calculated.

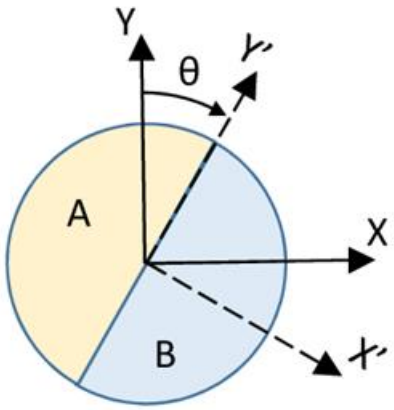

Figure 2. Reference directions and rotation angle for split target model.

Results from these model calculations for "fast" (10 rpm) target rotation are shown in Figures 3 to 6, using these model parameters: beam rastered ±10 cm starting from target center, target rotated at 10 rpm, and beam returns to target center after either 360° (Figures 3 and 4) or 540° (Figures 5 and 6) of target rotation (two different θ_1 values). Note that because the target rotation speed is constant, the plots of beam position versus target rotation angle can also be viewed as beam position versus time. Figures 3 and 5 are shown in the target frame of reference, while Figures 4 and 6 are shown in the laboratory frame of reference.

For the case of Figure 4, then, the time t_A spent by the beam on target side A is equal to the time t_B spent on target side B, whereas for Figure 6, the beam spends 3 times as much time on side A as on side B (over the course of two target rotations). For a given value of θ_2, the t_A:t_B ratio is determined by the θ_1 value selected. In this model, the pattern traced by the beam, and the t_A:t_B ratio, is repeated every two target rotations (for $\theta_2 = 720°$).

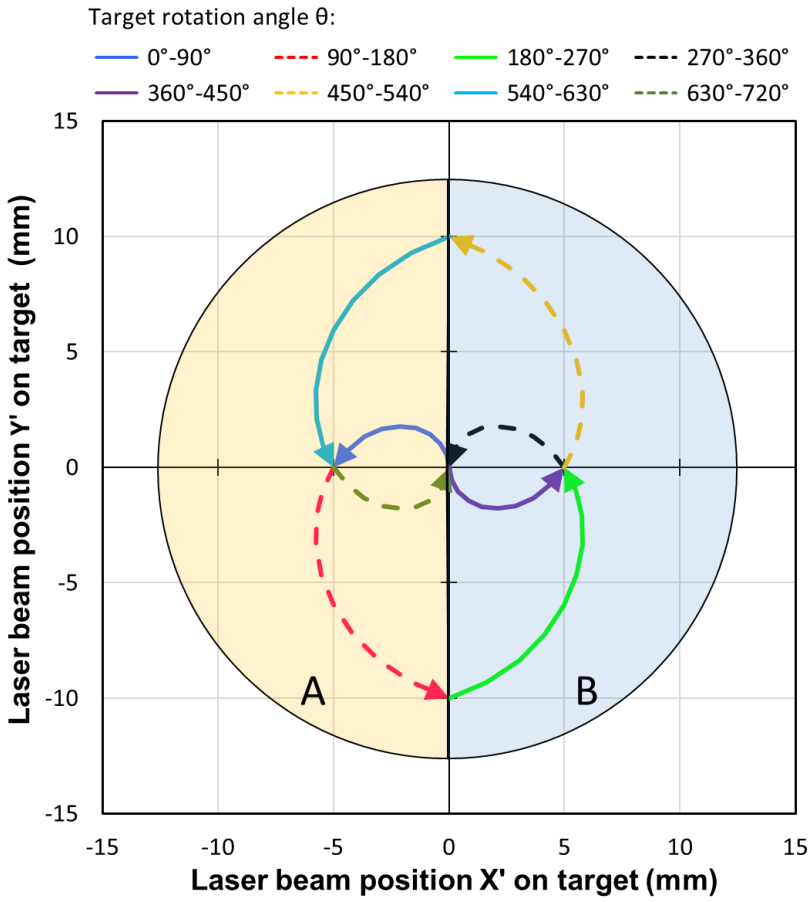

Figure 3. Calculated beam path Y' vs. X' ("fast" rotation, equal raster speeds).

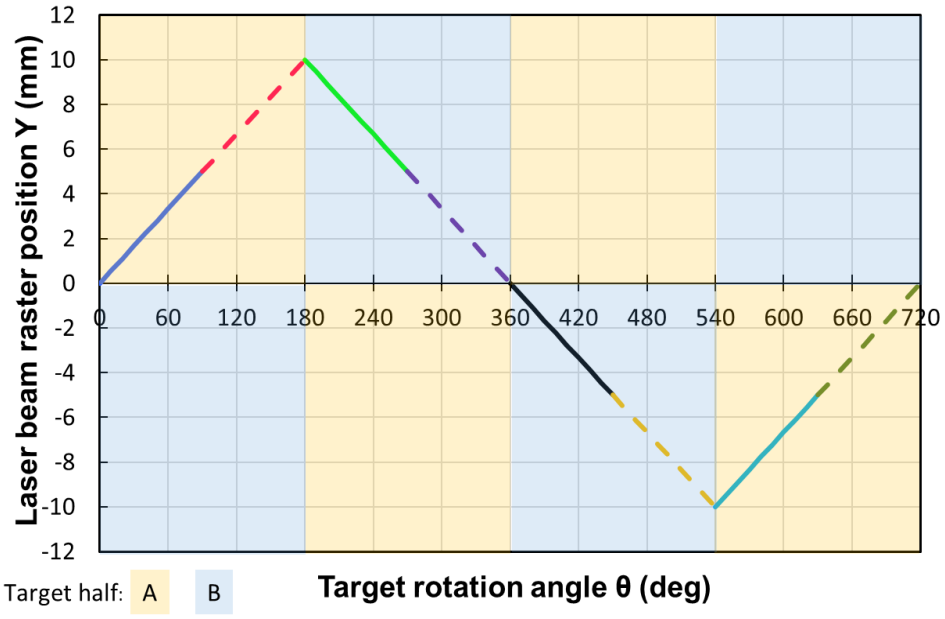

Figure 4. Calculated beam position Y vs. target rotation angle θ ("fast" rotation, unequal raster speeds).

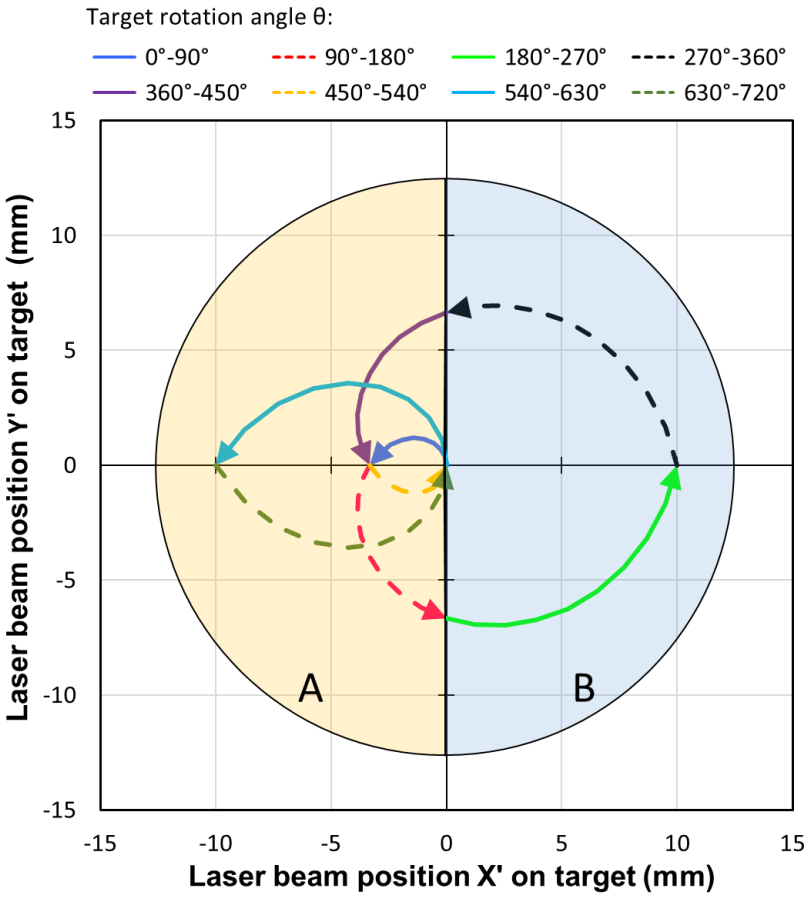

Figure 5. Calculated beam path Y' vs. X' ("fast" rotation, unequal raster speeds).

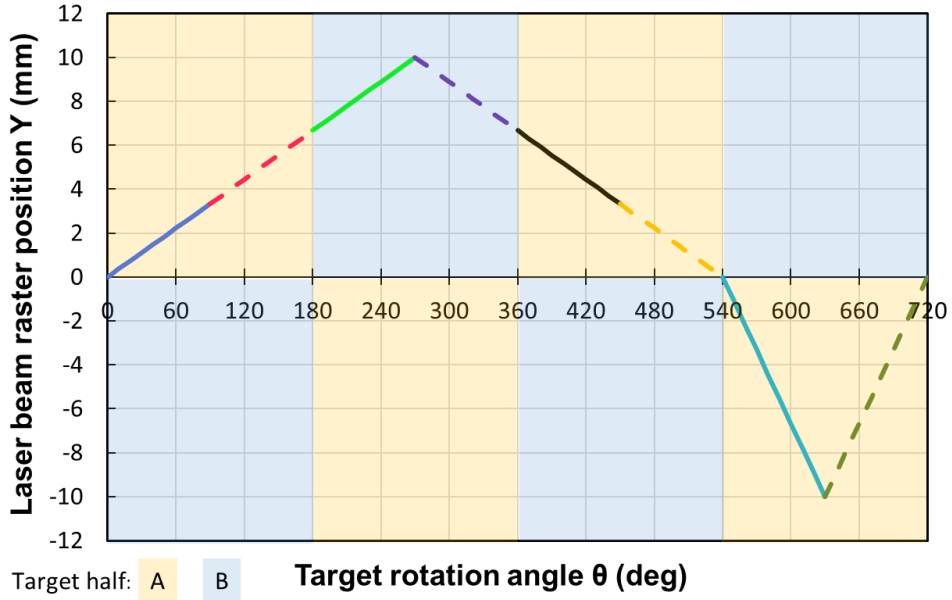

Figure 6. Calculated beam position Y vs. target rotation angle θ ("fast" rotation, unequal raster speeds).

The calculated dwell time fraction for each target side as a function of θ_1 is shown in Figure 7 (from 0 to 360°; the dwell time fraction values from 360 to 720° are equal to the 0 to 360° values). The dwell time fraction for side A is $t_A/(t_A+t_B)$, and similarly for side B.

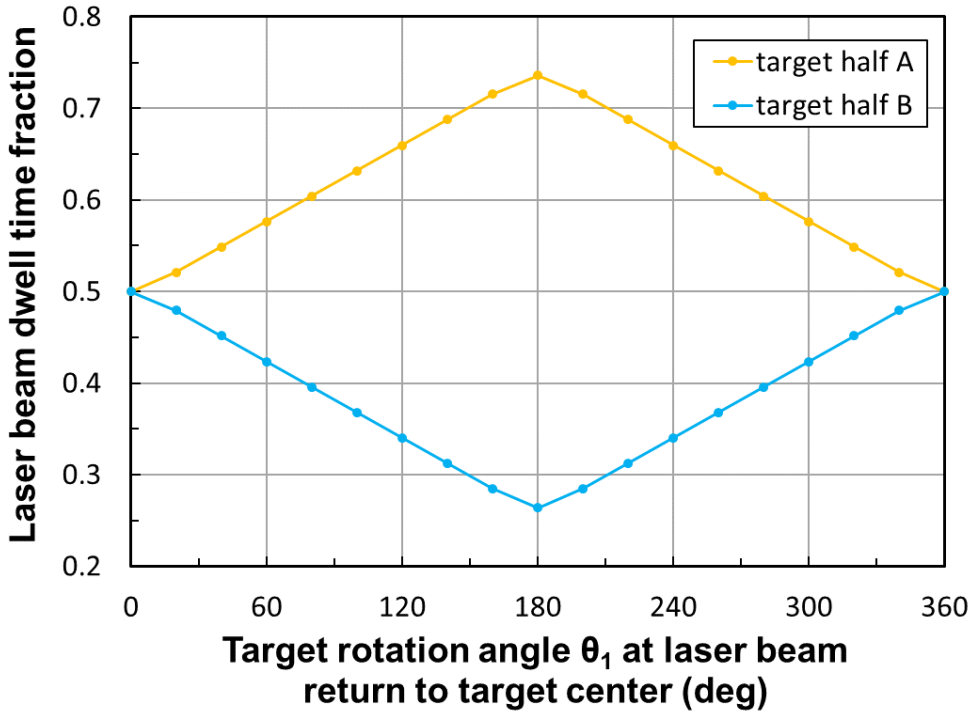

Figure 7. Calculated fraction of dwell time spent on each target half (see text).

On examination of Figures 3 and 5, another apparent drawback of the "fast" target rotation method is that, assuming that somehow the target rotation and beam raster motions remain synchronized, the target will be ablated only along the paths shown in these figures. That is, the target surface will not be ablated uniformly. In this case, most of the target surface will not be ablated, while over time a deep trench will be ablated along the calculated paths (thus wasting most of the target).

Actual film depositions using this "fast" rotation method, however, result in target surfaces that are uniformly ablated over the circle defined by the beam rastering. This result indicates that the ablated pattern, shown in Figures 3 and 5 for one beam raster cycle, slowly precesses around the target center, producing a complete solid circle ablation pattern on the target over the course of the deposition.

Model calculation results for the case of "slow" target rotation are shown in Figures 8 to 11. Figures 8 and 10 are shown in the target frame of reference, while Figures 9 and 11 are shown in the laboratory frame of reference. The model parameters for Figures 8 and 9 are: beam rastered ±10 cm starting from the target center, target rotated at 0.01 rpm over 132° giving an elapsed time of 37 minutes. The model parameters for Figures 10 and 11 are: beam rastered ±10 cm starting from the target center, target rotated at 0.005 rpm over 151° giving an elapsed time of 84 minutes. The beam rastering speeds v_A and v_B (on target sides A and B, respectively) for Figures 8 and 9 are $v_A \approx 0.2$ mm/s and $v_B \approx 0.1$ mm/s, while the values for Figures 10 and 11 are $v_A \approx 4.4$ mm/s and $v_B \approx 1.1$ mm/s. The results of Figures 8 and 9 are for illustration purposes only, with Figure 8 showing details of the beam path and Figure 9 showing how the beam spends twice as much time on target side B as on target side A ($v_A/v_B = 2$). Using more realistic values of v_A and v_B, Figures 10 and 11 show results that might be expected in the laboratory. The t_A:t_B ratio,and thus the elemental

composition of the deposited film, is determined by the v_A:v_B ratio selected. For the model parameters of Figure 11, the t_A:t_B ratio is equal to 4.

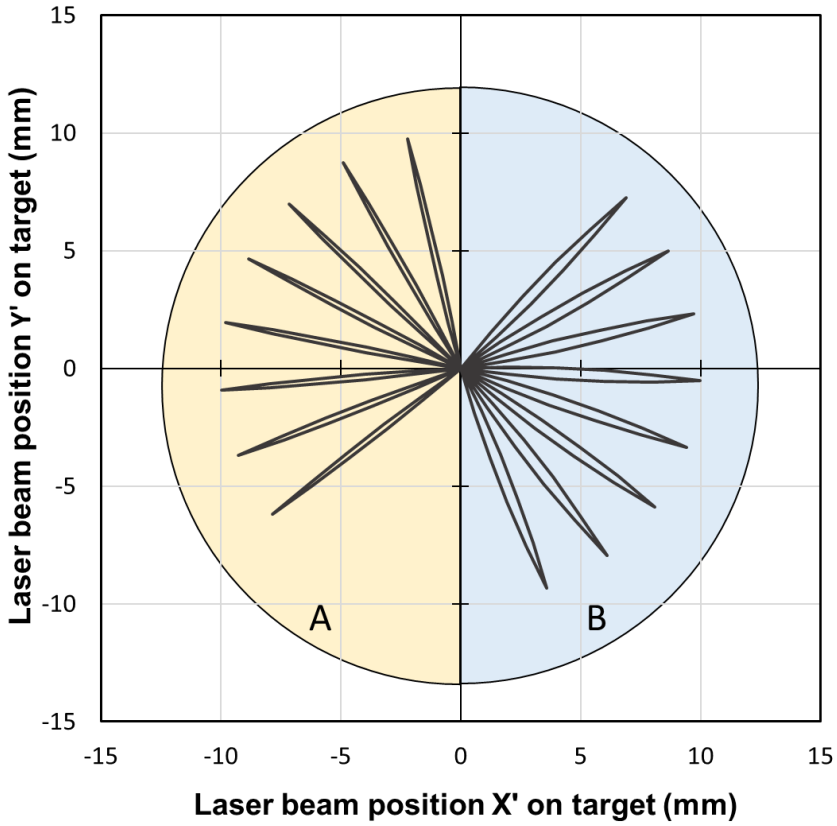

Figure 8. Calculated beam path Y' vs. X' ("slow" target rotation: 0.01 rpm).

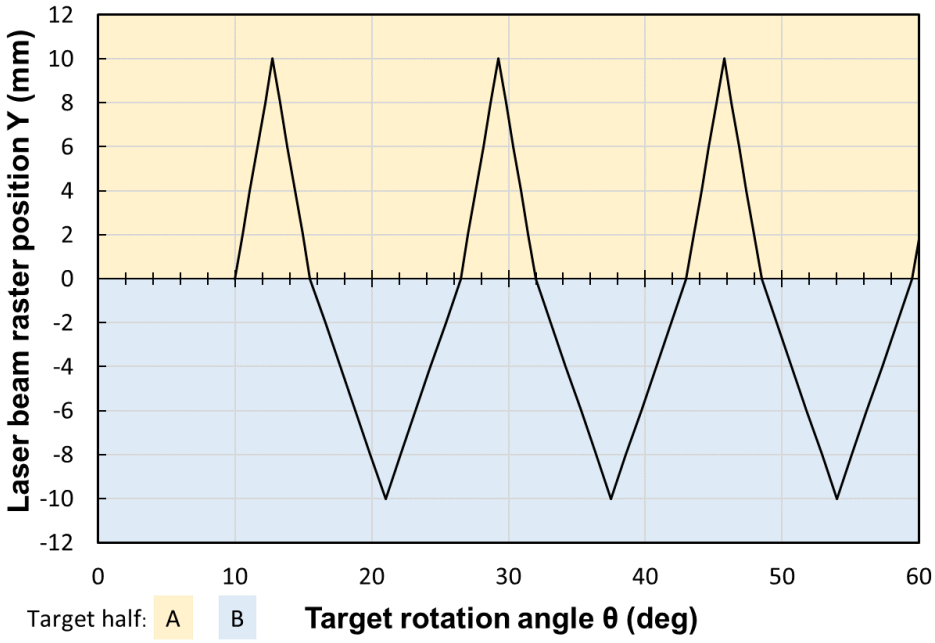

Figure 9. Calculated beam position Y vs. target rotation angle θ ("slow" target rotation: 0.01 rpm).

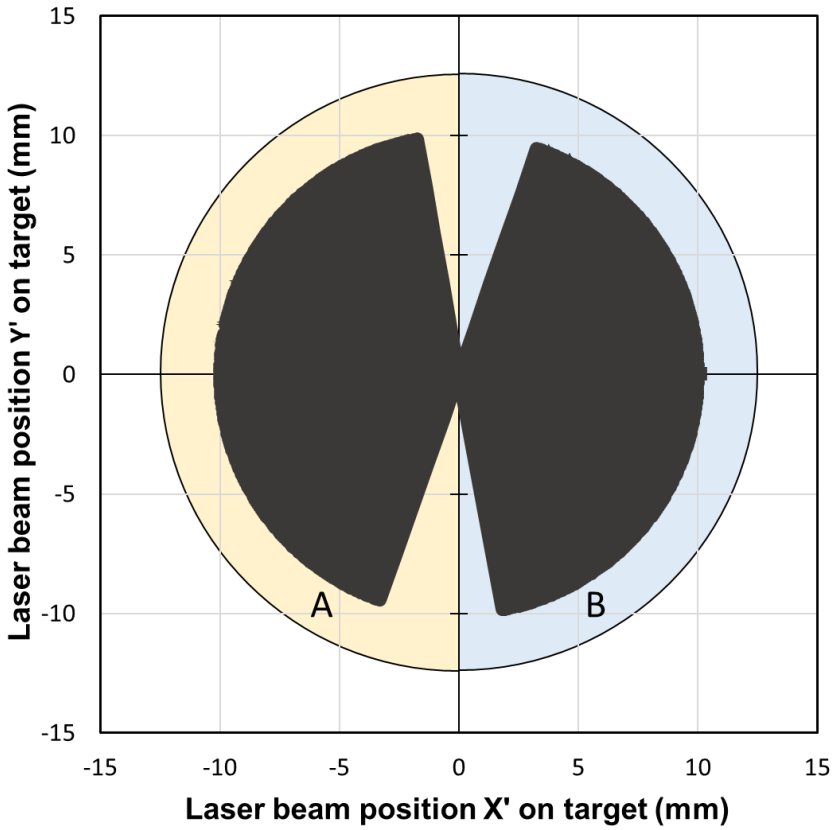

Figure 10. Calculated beam path Y' vs. X' (“slow” target rotation: 0.005 rpm).

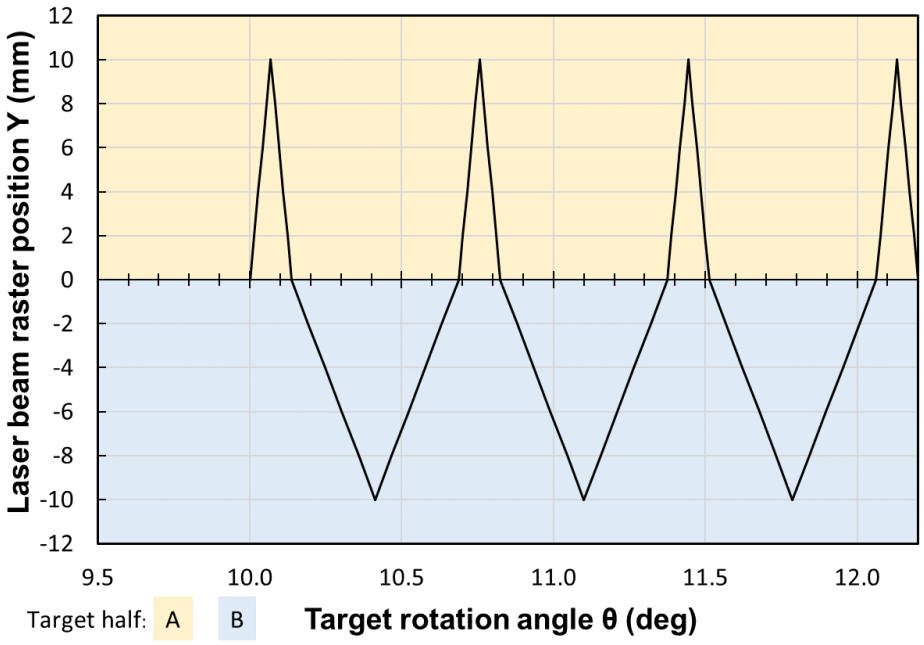

Figure 11. Calculated beam position Y vs. target rotation angle θ (“slow” target rotation: 0.005 rpm).

2.1.3 Target Preparation and Use

Two types of laser ablation targets were used to deposit the BDFO films described in this report: (1) single, uniform composition targets, and (2) split (half-and-half) composition targets. Both target types are 1-inch (25.4 mm) diameter disks (approximately 3 mm thick) made by hot-pressing an appropriate mixture of the constituent metal oxides (Bi_2O_3, Dy_2O_3, and Fe_2O_3, in the case of BDFO). The split targets consist of two semicircular disks indium-bonded side by side onto a copper backing plate, as shown in Figure 12. All targets were obtained from ACI Alloys, Inc.[3].

BDFO films with the elemental composition $Bi_{0.7}Dy_{0.3}FeO_3$ have been reported to have good multiferroic properties at room temperature [4]. The elemental compositions of the targets used to produce the BDFO films described here are listed in Table 1. Note that the composition of target TGT41 is the same as the desired film composition.

Table 1. Elemental composition of the laser ablation targets.

Target number:		TGT41	TGT42	TGT50		TGT61
Target type:		single	single	split		single
Target half:		—	—	A	B	—
Cation ratio	Bi	0.70	1.00	1.88	1.88	0.74
	Dy	0.30	0.30	0.72	0.71	0.09
	Fe	1.00	1.00	1.00	0.00	1.00
Cation percent	Bi	35.0	43.5	52.3	72.5	16.2
	Dy	15.0	13.0	19.9	27.5	1.9
	Fe	50.0	43.5	27.8	0.0	21.9

Figure 12. Split, 1-inch diameter ablation target TGT50 (Fe-rich half A at bottom).

2.2 BDFO FILMS

2.2.1 Growth Conditions

The BDFO films were deposited using a Nano-PLD-1000 pulsed laser deposition system, manufactured by PVD Products, Inc.,[5] and a Lambda Physik Compex 102 excimer laser (248 nm) [6]. The Nano-PLD chamber is outfitted with a six-target carousel with target rotation and rastering capability. The angle of incidence of the laser beam on the target is 60° with respect to the target normal. The laser beam is focused onto the ablation target using a projection optical train similar to that described by Dam, et al [7].

Before deposition, the PLD chamber was evacuated to a base pressure below 5×10^{-6} Torr. The films were typically deposited for one hour, in the presence of low pressure oxygen gas, onto Si (100) substrates at either ambient temperature or heated to several hundred degrees Centigrade. The deposition conditions for the various BDFO films discussed in this report are listed in Table 2, including the laser beam spot size and the laser fluence, or energy density, at the target surface. Films that were deposited at the same time (with multiple substrates loaded symmetrically on the rotating substrate holder) are grouped together in the table. The laser beam spot size was measured before film deposition by ablating a small piece of Kentek [8] ZAP-IT-G® photo-sensitive alignment paper (for FLM154) or Si wafer (for other films) placed on top of the ablation target. The Si wafer piece was ablated, at the laser deposition power level, for 100 pulses (PLD42-PLD65) or 10 pulses (PLD77-PLD79), while the Kentek paper was ablated for a single pulse at the lowest laser energy possible (corresponding to a laser power setting of 19 kV). Spot size values indicated by ditto marks in the table were assumed to be the same as those measured for the previously listed deposition (these depositions were performed on consecutive days).

2.2.2 Characterization

The elemental composition of the films was determined using either energy-dispersive spectroscopy (EDS) or wavelength-dispersive spectroscopy (WDS) with a scanning electron microscope. The ferroelectric properties of the films were characterized by measuring the electric polarization versus applied electric field (ferroelectric hysteresis curve) using a Precision LC instrument from Radiant Technologies, Inc. [9] Small surface contacts (100 μm × 100 μm) for the hysteresis measurements were deposited onto the BDFO film and photo-lithographically defined. Fine metal probes were used to connect the measuring instrument to these contacts.

Table 2. Deposition conditions for the deposited BDFO films.

Sample #	Target #	Target-to-substrate distance (cm)	O_2 pressure (mtorr)	Heater set-point	Target rotation speed (rpm)	Target conditioning time (min)	Laser beam spot size (mm^2)	Laser beam fluence (J/cm^2)	Fraction of time on side A	Deposition time (min)
PLD00	TGT42	—	—	690°C	30	0	not measured	not measured	N/A	—
PLD41 PLD42	TGT50	5.9	0.3	—	10	0	5.30	1.9	0.50	62
PLD47	TGT50	5.9	0.3	690°C	10	62	"	1.2	0.50	60
PLD64 PLD65	TGT50	5.9	0.3	690°C	0.005	0	1.58	3.1	0.50	60
PLD77 PLD78 PLD79	TGT50	5.9	0.3	—	0.0055	0	1.22	3.3	0.33	60
PLD81	TGT50	5.9	0.3	—	0.0055	0	not measured	not measured	0.20	80
PLD84	TGT50	5.9	0.3	—	0.005	0	not measured	not measured	0.80	75
PLD140	TGT61	5.9	15	—	10	30	2.09	3.1	N/A	15
PLD147	TGT61	5.9	15	690°C	10	30	"	2.5	N/A	60
PLD149	TGT61	5.9	15	600°C	10	30	"	3.1	N/A	60
PLD153 PLD154	TGT61	5.9	15	650°C	10	30	"	3.1	N/A	60

This page is intentionally blank.

3. RESULTS

3.1 BDFO FILMS

3.1.1 Film Elemental Composition

An initial BDFO film (PLD00) was deposited onto a heated (690°C) Si (100) substrate by ablation of single-composition target TGT42. Standard-less EDS measurement of the film's elemental composition indicated that the film is quite bismuth deficient relative to iron: $Bi_{0.155}Dy_{0.075}FeO_x$, compared to the desired $Bi_{0.7}Dy_{0.3}FeO_3$ composition (note that oxygen content cannot be reliably measured with the EDS technique). The measured Bi to Dy ratio of 0.70:0.34 is close to the desired value of 0.7:0.3. The composition of each half of split target TGT50 was then selected based on these analysis results, with the goal being to enable deposition of films with a wide range of Bi:Fe ratios and approximately correct Bi:Dy ratios.

The measured composition of films produced using targets TGT42, TGT50, and TGT61 are summarized in Table 3. For all listed films, the laser beam was rastered at a constant speed across the whole target (which was rotating at 10 rpm). For films PLD42 and PLD47, then, the laser beam dwell times on the two halves of TGT50 were equal. EDS measurements of these two films were performed using target half B of TGT50 as a known-composition standard (rather than the standard-less method used for PLD00).

The results of these standard-based measurements (presumed to be more accurate) cast doubt on the elemental composition results for PLD00 listed above (compare the measured Dy and Fe percentages of PLD00, relative to the target percentages, to those of PLD47). And because the composition of TGT50 was selected based on the measured PLD00 composition, the films produced using TGT50 (under the same deposition conditions as PLD00) are not be expected to have the desired $Bi_{0.7}Dy_{0.3}FeO_3$ composition (which is fact the case for PLD47, as shown in Table 2).

Film PLD42 was deposited at ambient temperature using split-composition target TGT50, with equal beam rastering speeds (and therefore equal beam ablation or dwell times) on each half of the target. The resultant elemental composition of film PLD42 is therefore expected to be an average of the composition of the two target halves. The measured composition for this film is within 2% or better of this expected composition. The target cation percent values for the split-composition targets listed in Table 3 are averages of the cation percent values for the target halves listed in Table 1 (an "effective" composition, as if the target had a single elemental composition).

Table 3. Elemental composition of the deposited BDFO films.

Film	Target	Heater set-point	Effective target cation %			Measured cation %			Film analysis method
			Bi	Dy	Fe	Bi	Dy	Fe	
PLD00	TGT42	690°C	43.5	13.0	43.5	12.6	6.1	81.3	EDS
PLD41	TGT50	—	62.4	23.7	13.9	71.8	24.3	3.9	WDS
PLD42	TGT50	—	62.4	23.7	13.9	62.3	23.6	14.1	EDS
PLD47	TGT50	690°C	62.4	23.7	13.9	41.4	45.5	13.1	EDS
PLD48	TGT50	690°C	62.4	23.7	13.9	36.8	53.6	9.6	WDS
PLD64	TGT50	690°C	62.4	23.7	13.9	31.0	54.5	14.5	EDS
PLD65	TGT50	690°C	62.4	23.7	13.9	28.7	59.9	11.4	WDS
PLD77	TGT50	—	62.4	23.7	13.9	73.6	24.0	2.5	WDS
PLD78	TGT50	—	62.4	23.7	13.9	69.9	25.4	4.7	EDS
PLD79	TGT50	—	62.4	23.7	13.9	73.7	23.8	2.5	WDS
PLD81	TGT50	—	62.4	23.7	13.9	73.5	24.2	2.3	WDS
PLD84	TGT50	—	62.4	23.7	13.9	68.9	23.3	7.8	WDS
PLD140	TGT61	—	40.5	4.7	54.8	54.6	1.7	43.6	WDS
PLD147	TGT61	690°C	40.5	4.7	54.8	11.4	3.1	85.5	WDS
PLD149	TGT61	600°C	40.5	4.7	54.8	33.4	3.4	63.1	WDS
PLD153	TGT61	650°C	40.5	4.7	54.8	19.7	3.7	76.6	WDS
PLD154	TGT61	650°C	40.5	4.7	54.8	—	—	—	—

3.1.2 Effect of Substrate Temperature

Film PLD47 was deposited under the same conditions as for film PLD42, but at an elevated substrate temperature of 690°C. As expected, the percentage of Bi relative to Fe is lower than that for ambient temperature deposition (see the PLD42 and PLD47 results in Table 3) because Bi is more volatile than Fe at elevated temperatures. Unexpectedly, however, the same does not hold true for the percentage of Dy relative to Fe (Dy is also more volatile than Fe at high temperatures). This inconsistency may be due to the fact that the EDS method of measuring the film elemental composition cannot easily distinguish between Dy and Fe x-ray peaks, which overlap (see, for example, the Dy and Fe spectral peaks at about 6.5 kV in Figure 13). BDFO films PLD64 and PLD65 of this figure were produced during the same deposition and so should have essentially identical elemental compositions.

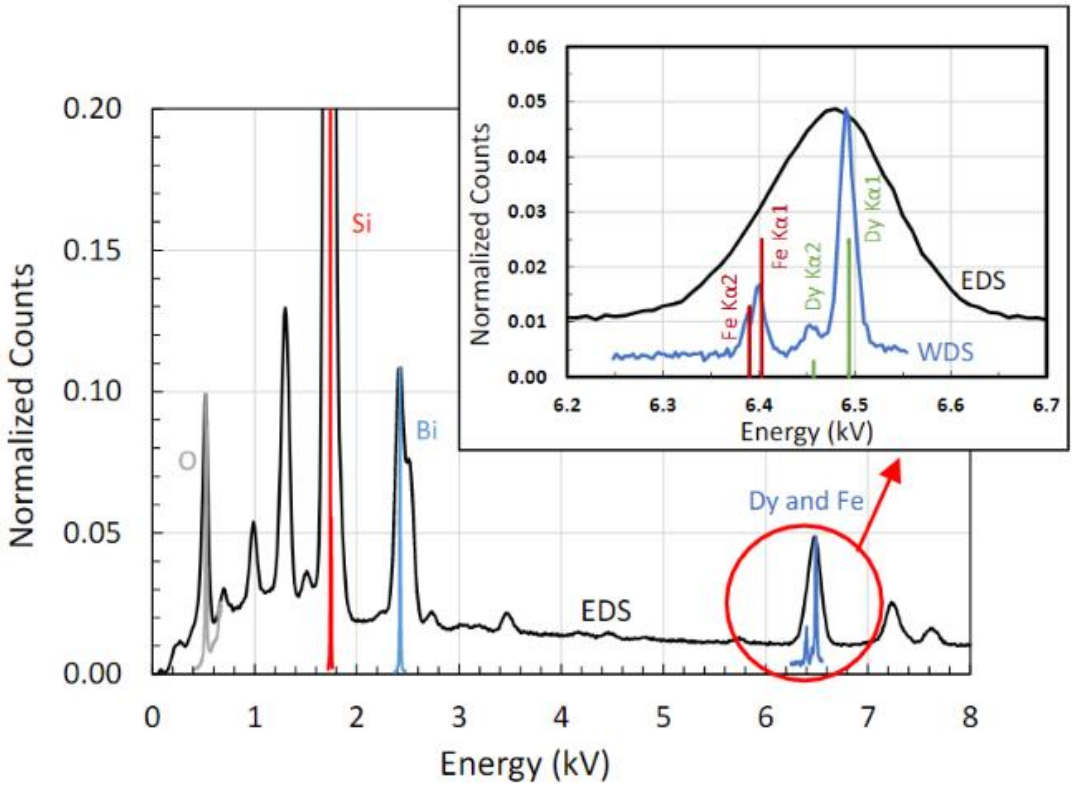

Figure 13. Comparison of EDS and WDS spectra for BDFO films PLD64 (EDS) and PLD65 (WDS).

The effect of substrate temperature on the Bi:Fe and Dy:Fe ratios is more clearly seen in Figure 14, where these atomic ratios, as measured by WDS, are plotted versus temperature for BDFO films that were ablated using the same ablation target. The dashed lines are guides to the eye.

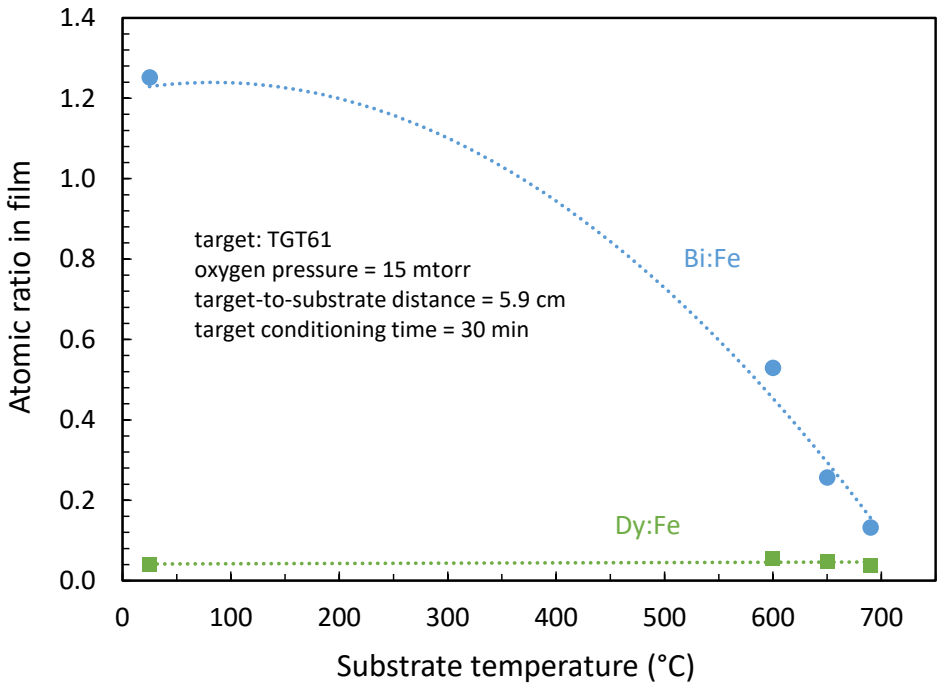

Figure 14. Film atomic ratio relative to Fe versus substrate temperature.

3.1.3 Effect of Time Fraction Spent on Each Side of Split-Composition Targets

The expected (calculated) Fe:Bi ratio for films deposited from split-composition target TGT50 (assuming that all elements are ablated equally from the target and stick equally well to the substrate) is shown in Figure 15 as a function of the fraction of time that the laser beam spends on the Fe-rich side (side A) of the target. Also shown in the figure are WDS-measured Fe:Bi ratios of several films (PLD41, PLD77, PLD79, PLD81, and PLD84) deposited at ambient temperature from TGT50 (which was "sanded" with a polymer abrasive pad and cleaned with methanol prior to each deposition to ensure the same starting target composition for all films).

Another way of looking at the effect of the fraction of time that the laser beam spends on a given side of the ablation target is shown in Figure 16 (for the same films with data shown in Figure 15). In this case, the atomic percent of the individual elements is plotted relative to the atomic percent for that element in the Fe-poor side of target TGT50. The lines in this figure and subsequent figures are fits to the data to guide the eye. As seen, the amount of Dy in the films is relatively constant, while the Fe content goes up and the Bi content goes down as a higher fraction of time is spent ablating the Fe-rich side of the target.

From Figure 15 in particular, one can see that the Fe:Bi ratio in the films does not increase as much as expected as a higher fraction of time is spent ablating the Fe-rich side of the split-composition target. Because the films represented in Figures 15 and 16 were deposited at ambient temperature, any Bi, Dy, and Fe atoms ablated from the target that reach the substrate are expected to stick to the substrate. So, with respect to Bi and Fe, either these atoms are not ablated from the target at an equal rate (i.e., they are ablated incongruently), or, once ablated, do not arrive at the substrate at an equal rate (or some combination of these two effects). The relative importance of these effects, as

well as unequal sticking coefficients of Bi and Fe when deposited onto heated substrates, will be discussed in more depth below and in a subsequent publication.

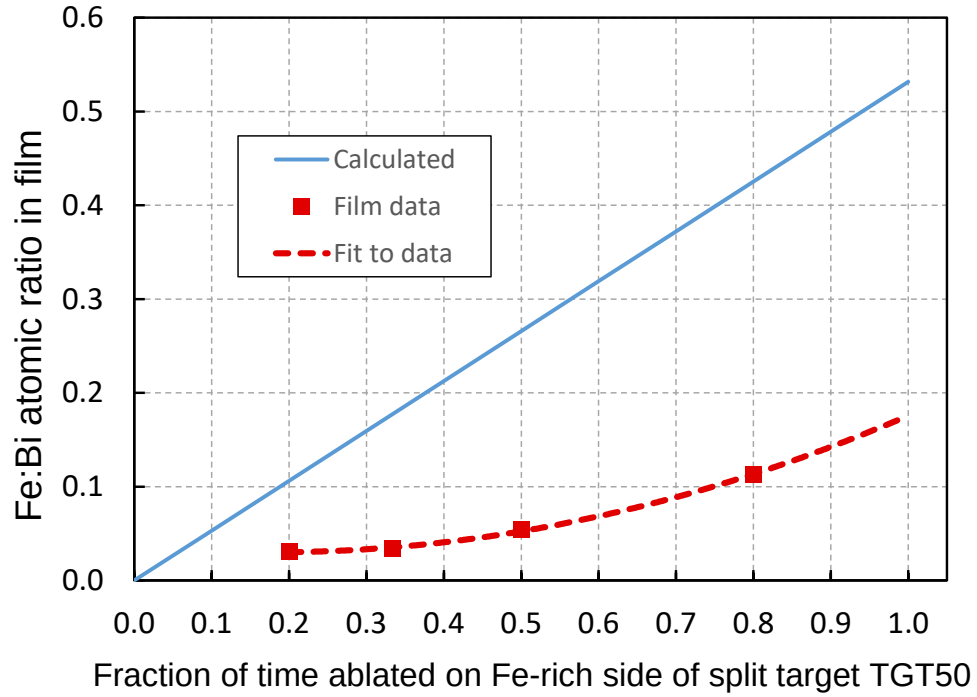

Figure 15. Calculated and measured Fe:Bi ratio for films deposited with a split-composition target.

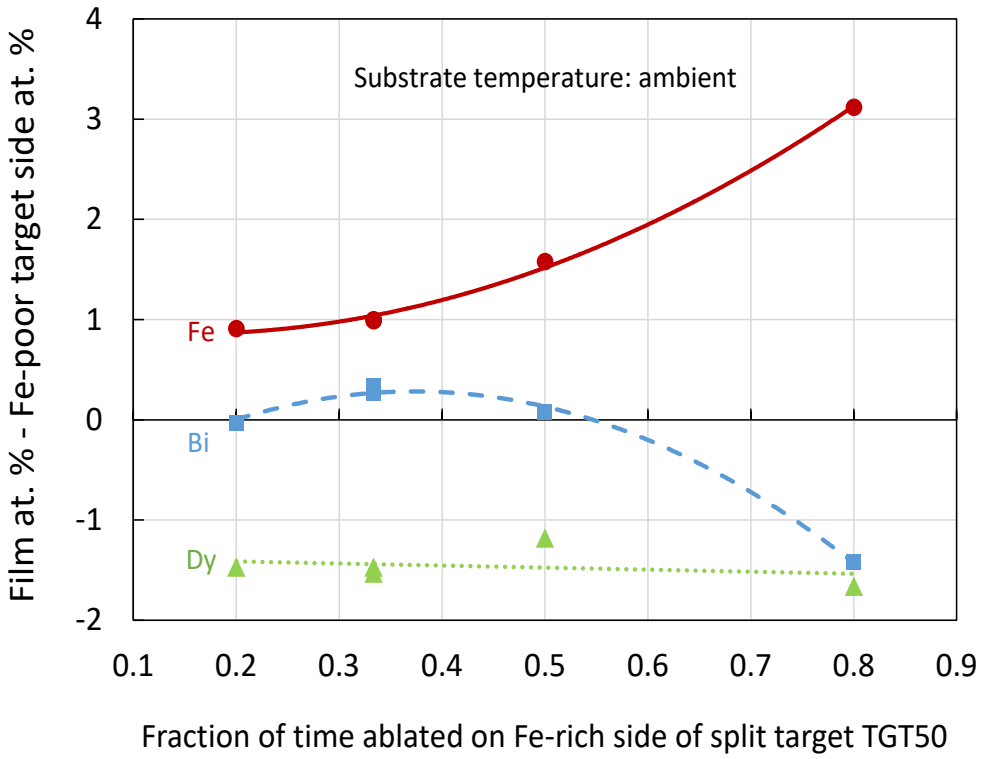

Figure 16. Film elemental composition relative to Fe-poor side of TGT50.

Figure 17 illustrates these effects as well as other aspects of film deposition when using a multi-element, split-composition ablation target. EDX analysis results for BDFO film PLD78, deposited onto an ambient temperature Si substrate from split-target TGT50, are shown in the figure. First, for this film, the laser beam raster speed was adjusted, mid-raster, so that the beam spent twice as much time on the Fe-poor side of the target (half A) as on the Fe-rich side (half B) of the target. In the figure, the cation percentages for target halves A and B are shown as solid and dashed lines, respectively. The dotted lines represent an "effective" target composition (the expected film composition) for the particular beam raster speed settings used. Note, for example, that the percentage of Dy in the film is about 2/3 of the way between the target half B Dy percentage and the target half A Dy percentage, as expected based on the time that the laser beam spent on each target half (i.e., the film Dy data points lie on the dotted Dy line).

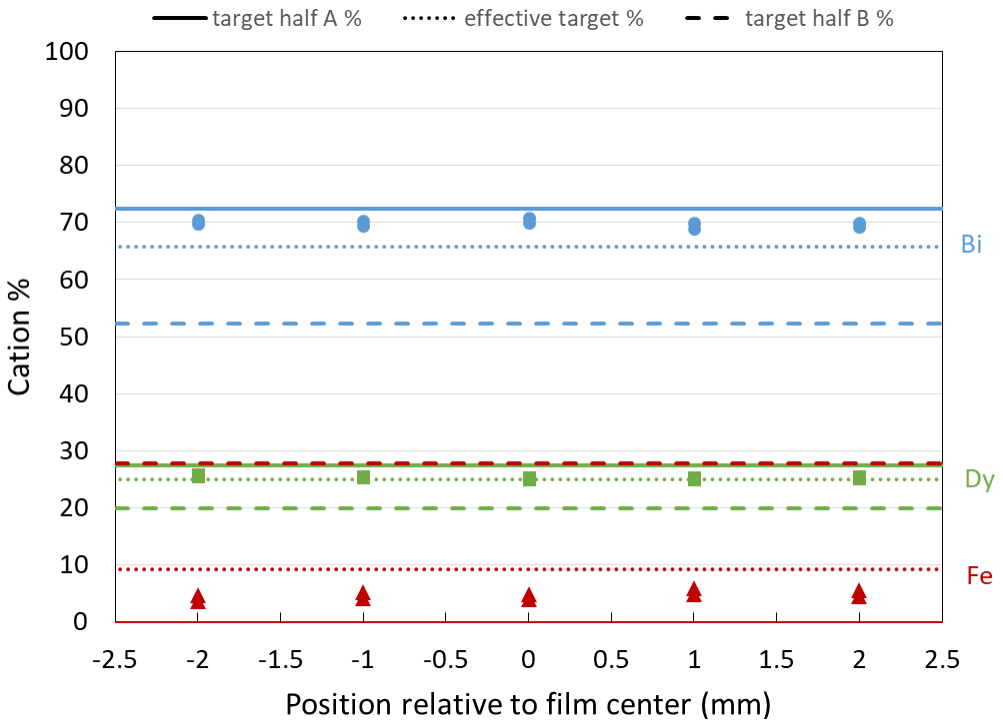

Figure 17. Film cation percent (data points) as a function of distance from film center.

Second, the film composition was measured at various positions on the film surface, and plotted in the figure versus the distance from the film center. As seen, at least over a distance of 4 mm, the film has a uniform composition across its surface. There are two data points at each measurement position, corresponding to the use of calibration measurements taken at two different points on the calibration standard (TGT47, which has the same composition as half B of TGT50). The EDX measurements thus appear to be repeatable.

Third, the film contains more Bi than expected, and less Fe than expected (note the data points of the cation percent values of Bi and Fe relative to the dotted lines for those elements), in agreement with the results shown in Figure 15. Because the film is deposited onto an ambient temperature substrate, any cations ablated from the target are expected to stick to the substrate and form the composite BDFO film. The measured film Bi and Fe percentages suggest incongruent ablation of these elements from the ablation target. Although laser ablation is often touted as a means to produce

films with the same composition as the target, this is not strictly the case, especially when the elements in the target vary widely in volatility [10, 11, 12]. The melting temperature of Bi (271°C) is much lower than that of Fe (1538°C), while Dy has a somewhat lower melting point (1412°C) than Fe. As laser ablation using ns-width pulses is a thermal process, it's not surprising that Bi is much more easily ablated than either Dy or Fe, and that Dy is more easily ablated than Fe.

3.1.4 Effect of Target Conditioning Time

Due to the target element volatility effects described earlier, the composition of the surface layer of the ablation target will vary with time as the more volatile elements are preferentially ablated relative to the less volatile elements [13]. This surface layer, with a thickness determined by the interaction depth of the laser beam with the target, will eventually reach a steady-state composition [10, 11, 14, 15].

The measured composition of a series of BDFO films, ablated from the same target but with different pre-deposition target conditioning times, is shown in Figure 18. Note that the composition trends of the films will be the same as those of the target surface layer. For example, as the target conditioning time increases, the amount of Bi in the target will decrease relative to Dy and Fe (becoming Bi-poor, and Dy- and Fe-rich), and so the relative amount of Bi that ends up in the film will also decrease over time (because the target surface has become relatively Bi-poor).

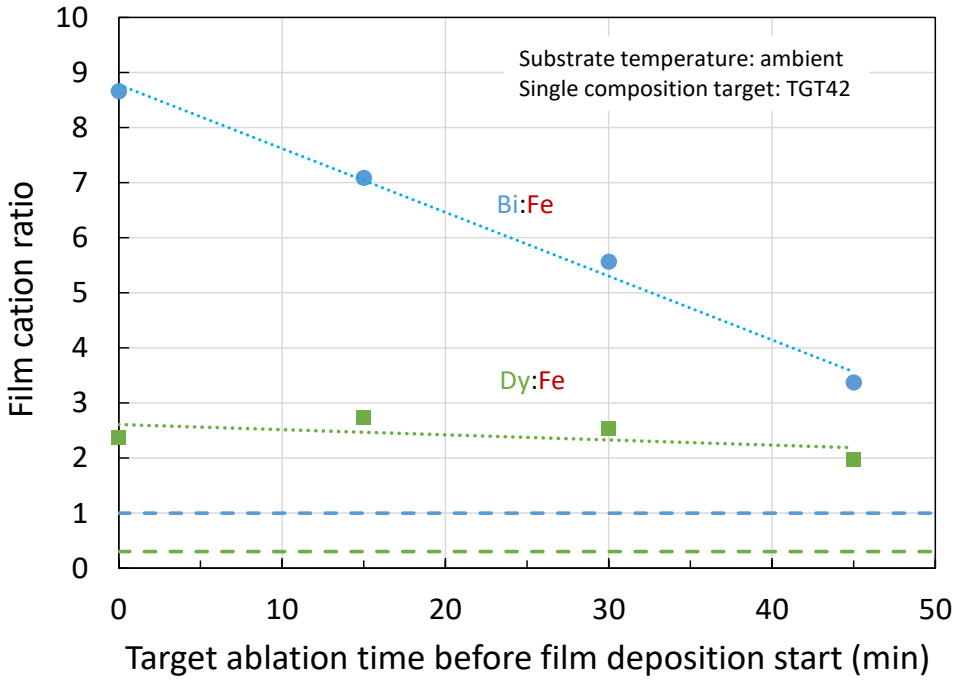

Figure 18. Film composition versus ablation target conditioning time

3.1.5 Effect of Laser Beam Fluence

As discussed above in section 3.1.2, the laser fluence (energy density) on the target may not be quite high enough to ablate all target elements equally, leading to preferential ablation of Bi and Dy compared to Fe. This effect is shown in Figures 19 and 20 for a series of BDFO films (PLD123, PLD127, PLD131, PLD135, and PLD139) all deposited from the same ablation target (TGT42).

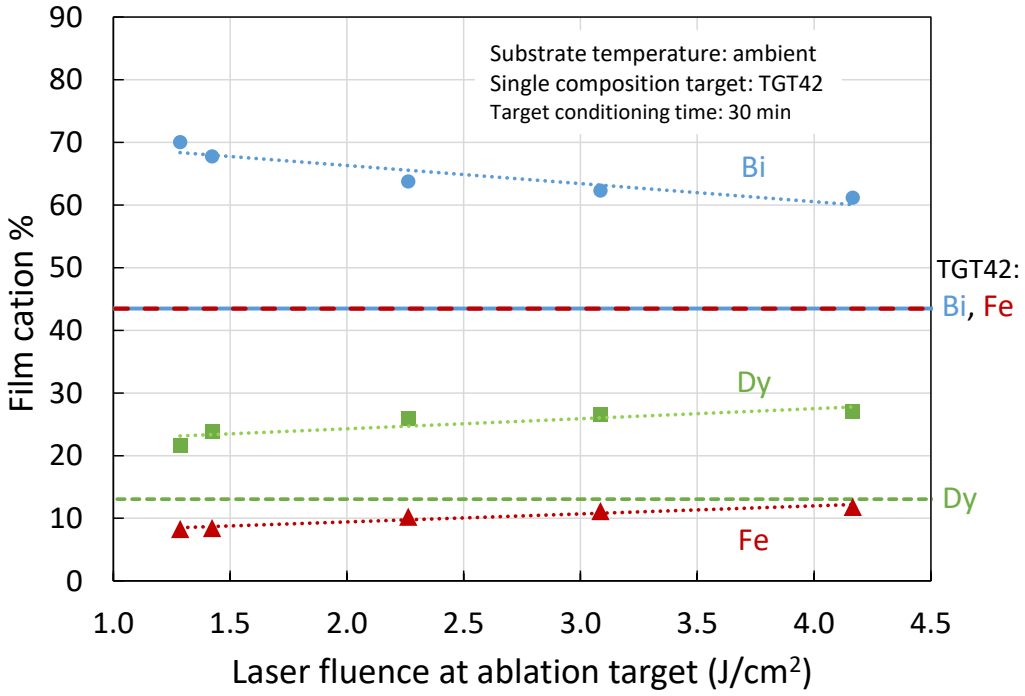

Figure 19. Film cation percent versus laser fluence.

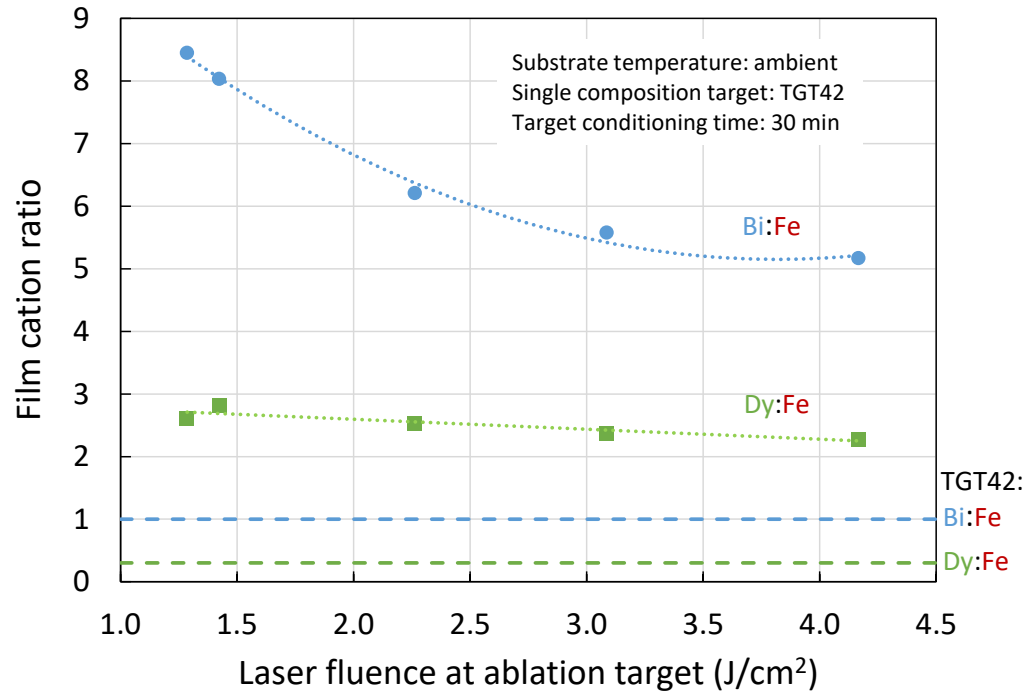

Figure 20. Film Bi:Fe and Dy:Fe ratios versus laser fluence.

Before the deposition of each of these films, the target was “sanded” and cleaned, as described earlier, and ablated (conditioned) for 30 minutes (to avoid target conditioning effects). The target cation ratios and percentages shown in the figures are those of the sanded/cleaned target (before conditioning). As seen in Figure 20, the films contain more Bi and Dy, relative to Fe, than the target (as expected because of the higher volatility of Bi and Dy compared to Fe). Note also that the Bi:Fe and Dy:Fe ratios decrease as the laser fluence increases. This behavior can be understood as the ablation rate (atoms ablated per laser pulse) of Fe, relative to that of Bi, for example, increasing with increasing fluence. One way for this to happen is if the Bi ablation rate is constant for fluences above about 1 J/cm^2 (i.e., all Bi atoms at the target surface are ablated, over the full range of studied fluences), while the less-volatile Fe atoms at the target surface are incompletely ablated at the lower fluences. If the ablation rate of Fe then increases with increasing fluence, the Bi:Fe ratio in the film will decrease. Because the substrates are at ambient temperature, any ablated target atoms that reach the substrate are assumed to stick to the substrate.

3.1.6 Ferroelectric Characteristics

The electrical hysteresis curve of BDFO film PLD154 (deposited using slightly Bi-rich, single composition target TGT61) is shown in Figure 21. The highly-doped silicon substrate for this film was used as a bottom electrode. From this hysteresis curve, the film appears to be ferroelectric, a first step in producing multiferroic films.

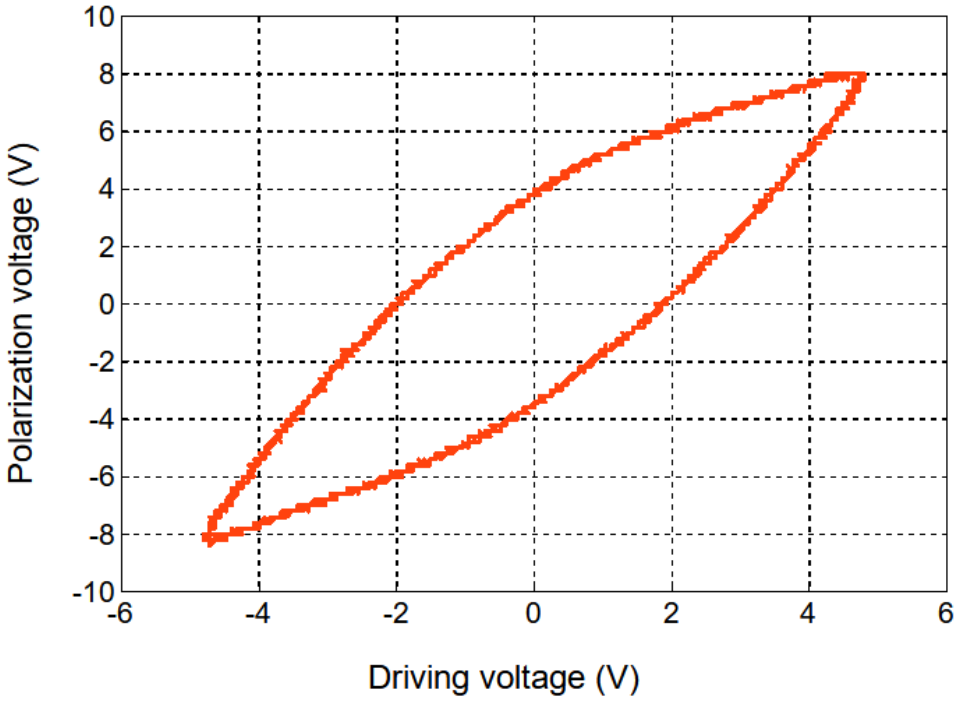

Figure 21. Ferroelectric hysteresis loop of BDFO film PLD154.

This page is intentionally blank.

4. SUMMARY AND CONCLUSIONS

With planned application to a magnetic field sensor, a simple means of controlling the elemental composition of multiferroic BDFO films has been demonstrated using pulsed laser deposition. Using a conventional single-composition target, the film composition can be difficult to control, particularly at elevated substrate temperatures, when the target contains some elements that are relatively more volatile than others.

The method described in this report uses a split-composition ablation target that is rotated about its center (to maximize target usage or coverage, and to more uniformly ablate the target surface) combined with variable speed laser beam rastering across the target. By using different raster speeds over the course of the raster cycle, the beam can spend more time on one half of the split target than on the other half. One half of the split target contains more of the most volatile elements (Bi and Dy for BDFO films) being deposited than the other half. By having the beam spend relatively more time on the volatile-element-rich half of the target, more of those volatile target atoms will make their way to the substrate, compensating for loss of that element in the deposited film due to evaporation from the substrate.

This film composition control technique was demonstrated by both simple model calculations of the laser beam raster position versus time (from which the beam dwell times were calculated) and by measurement of the elemental composition of a series of BDFO films deposited with various beam raster settings. Electrical hysteresis measurements show that the initial films are ferroelectric, despite having non-optimal elemental composition for multiferroic behavior.

Future work includes controlling the elemental and structural composition of deposited thin films by using a radio frequency (rf) plasma-assisted pulsed laser deposition technique. The addition of an rf discharge to the PLD system allows for tuning of the deposited layer's crystalline phase and orientation, dependent on the specific type and energy of the species involved in the discharge (oxygen, nitrogen) [16, 17]. The technique has been demonstrated to be effective for nanosecond (ns) PLD [18]. Its use in the femtosecond (fs) and picosecond (ps) regimes is completely unexplored, and can provide important insight into the ultrashort time scale of target/laser-beam interaction and on film growth mechanisms.

This page is intentionally blank.

REFERENCES

1. Khomskii, D. [2009] Classifying multiferroics: Mechanisms and effects, Physics, 2:20-27.
2. McGinnis, W. C., A. Hening, and T. Emery-Adleman [2020] System and Method for Controlling the Elemental Composition of Films Produced by Pulsed Laser Deposition, U.S. Patent 10676814 B2.
3. ACI Alloys, Inc., San Jose, CA, USA, https://www.acialloys.com/.
4. Prashanthi, K., B. A. Chalke, K. C. Barick, A. Dasc, I. Dhimanc, and V. R. Palkar [2009] Enhancement in multiferroic properties of $Bi_{0.7-x}La_xDy_{0.3}FeO_3$ system with removal of La, Solid State Commun., 149:188-191.
5. PVD Products, Inc., Wilmington, MA, USA, http://www.pvdproducts.com/.
6. Coherent, Inc., Santa Clara, CA, USA, https://www.coherent.com/.
7. Dam, B., J. Rector, M.F. Chang, S. Kars, D.G. de Groot, and R. Griessen [1995] The laser ablation threshold of YBa2Cu3O6+x, Appl. Surf. Sci., 86:13-17.
8. Kentek Corporation, Pittsfield, NH, USA, https://www.kenteklaserstore.com/.
9. Radiant Technologies, Inc., Albuquerque, NM, USA, https://www.ferrodevices.com/.
10. Chan, W.-T., X. L. Mao, and R. E. Russo [1992] Differential Vaporization during Laser Ablation/Deposition of Bi-Sr-Ca-Cu-O Superconducting Materials, Appl. Spectroscopy 46(6):1025-1031.
11. Arnold, C. B. and M. J. Aziz [1999] Stoichiometry issues in pulsed-laser deposition of alloys grown from multicomponent targets, Appl. Phys. A, 69(Suppl.):S23-S27.
12. Havelia, S., S. Wang, M. Skowronski, and P. A. Salvador [2009] Controlling the Bi content, phase formation, and epitaxial nature of $BiMnO_3$ thin films fabricated using conventional pulsed laser deposition, hybrid pulsed laser deposition, and solid state epitaxy, J. Appl. Phys., 106:123509.
13. Omori, N. and M. Inoue [1992] Excimer laser ablation of inorganic materials, Appl. Surf. Sci., 54:232-236.
14. Andreouli, C., T. Efthimiopoulos, S. Christoulakis, A. Tsetsekou, and C. Panagopoulos [2004] Influence of irradiated target modification on the quality of pulsed laser deposited $YBa_2Cu_3O_{7-x}$ thin films, J. Eur. Cer. Soc., 24:3623-3634.
15. Doeswijk, L. M., G. Rijnders, and D. H. A. Blank [2004] Pulsed laser deposition: metal versus oxide ablation, Appl. Phys. A, 7:263-268.
16. Teodorescu, M., M. Bazavan, E. R. Ionita, and G. Dinescu [2012] Characterization of an argon radiofrequency plasma jet discharge continuously passing from low to atmospheric pressure, Plasma Sources Sci. Technol., 21(5):055010.
17. Scarisoreanu, N. D., Dinescu M., and Craciun F. [2014] Multifunctional Oxides Obtained by PLD: Applications as Ferroelectric and Piezoelectric Materials, in Lasers in Materials Science, Springer Series in Materials Science, Castillejo, M., Ossi P., and Zhigilei L. (eds.), 191:227-269.
18. Gerhard, C., W. Viöl, and S. Wieneke [2016] Plasma-Enhanced Laser Materials Processing, in Plasma Science and Technology, Progress in Physical States and Chemical Reactions, Mieno, T. (ed.), DOI: 10.5772/61567, Ch. 1:3-23.

This page is intentionally blank.

INITIAL DISTRIBUTION

84310	Technical Library/Archives	(1)
71780	W. C. McGinnis	(1)
55360	A. Hening	(1)
71780	T. Emery-Adleman	(1)

Defense Technical Information Center
Fort Belvoir, VA 22060–6218 (1)

This page is intentionally blank.

REPORT DOCUMENTATION PAGE

Form Approved
OMB No. 0704-01-0188

PLEASE DO NOT RETURN YOUR FORM TO THE ABOVE ADDRESS.

1. REPORT DATE *(DD-MM-YYYY)*	2. REPORT TYPE	3. DATES COVERED *(From - To)*
January 2022	Final	

4. TITLE AND SUBTITLE

Advanced Electronic Films Using Pulsed Laser Deposition:
Multi-component Film Composition Control

5a. CONTRACT NUMBER

5b. GRANT NUMBER

5c. PROGRAM ELEMENT NUMBER

6. AUTHORS

Wayne C. McGinnis
Alexandru Hening
Teresa Emery-Adleman
NIWC Pacific

5d. PROJECT NUMBER

5e. TASK NUMBER

5f. WORK UNIT NUMBER

7. PERFORMING ORGANIZATION NAME(S) AND ADDRESS(ES)

NIWC Pacific
53560 Hull Street
San Diego, CA 92152–5001

8. PERFORMING ORGANIZATION REPORT NUMBER

TR-3258

9. SPONSORING/MONITORING AGENCY NAME(S) AND ADDRESS(ES)

NIWC Pacific In-House Innovation Program
53560 Hull Street
San Diego, CA 92152-5001

10. SPONSOR/MONITOR'S ACRONYM(S)

NIWC Pacific IIP

11. SPONSOR/MONITOR'S REPORT NUMBER(S)

12. DISTRIBUTION/AVAILABILITY STATEMENT

DISTRIBUTION STATEMENT A: Approved for public release. Distribution is unlimited.

13. SUPPLEMENTARY NOTES

14. ABSTRACT

A simple means of controlling the elemental composition of multiferroic Bi-Dy-Fe-O (BDFO) films has been demonstrated using a split pulsed laser ablation target that is rotated about its center, combined with variable speed laser beam rastering across the target. This film composition control technique was demonstrated by both simple model calculations of the laser beam raster position versus time and by measurement of the elemental composition of a series of BDFO films deposited with various beam raster settings. Electrical hysteresis measurements show that the initial films are ferroelectric, despite having non-optimal elemental composition.

15. SUBJECT TERMS

pulsed laser deposition; multiferroic; thin films; laser ablation; bismuth; dysprosium; iron; oxide

16. SECURITY CLASSIFICATION OF:			17. LIMITATION OF ABSTRACT	18. NUMBER OF PAGES	19a. NAME OF RESPONSIBLE PERSON
a. REPORT	b. ABSTRACT	c. THIS PAGE			Wayne McGinnis
U	U	U	SAR	44	19B. TELEPHONE NUMBER *(Include area code)* (619) 553-5610

Standard Form 298 (Rev.
Prescribed by ANSI Std. Z39.18

This page is intentionally blank.

This page is intentionally blank.

Naval Information Warfare Center Pacific (NIWC Pacific)
San Diego, CA 92152-5001